Mechanics of Advanced Composite Structures 9 (2022) 185 – 197

Semnan University

Mechanics of Advanced Composite Structures

journal homepage: http://MACS.journals.semnan.ac.ir

Strengthening of One-Way Slabs Using Composite Laminates of HPFRCC Including Synthetic Fibers PPS

A. Kheyroddin, Z. Madah*, M. Arab Hasanabade

Department of Civil Engineering, Semnan University, Semnan, Iran

KEYWORDS

One-way reinforced concrete slab;
Synthetic fibers;
Near-surface mount method (NSM);
Fiber-Reinforced Concrete Composite (HPFRCC).

ABSTRACT

Some available One-Way reinforced concrete slabs show weak structural performance due to reduced flexural capacity and environmental deterioration. Some of these buildings and bridges have been severely damaged due to natural disasters such as earthquakes, fatigue of materials, and so on. Therefore, repairing and strengthening these structures using modern materials (such as high-performance composites) which have quite similar behavioral characteristics to concrete, can be vital and economical. In addition, it has other characteristics, including strain hardening behavior under tension and affordable cost. In this study, the behavior of slabs reinforced with precast Laminates of High-Performance Fiber-Reinforced Concrete Composite (HPFRCC) made of synthetic fibers was investigated with the help of full-scale test models and near-surface mount method (NSM). For this purpose, 12 specimens of the one-way slab were constructed. In the construction of these specimens, it has been used the same mixed design with characteristic strength f'c=21 MPa in accordance with the ACI318 regulation. Their dimensions are 1200×500 ×100 mm. A reinforced slab with four bars (No.8) in the tensile area was considered as the normal reference slab. The rest of the slab was weakened by reducing 50% of the tensile bars. Among weak slabs, a slab was defined as a reference slab and the other 10 slabs were reinforced with HPFRCC Laminates in the tension area. Composite Laminates were attached to the slab by epoxy grout and using the NSM method. All slabs were evaluated by a pure one-point bending test after preparation. Forces and displacements were recorded during the test process and the situation of cracks was examined. The results of this study indicated that the flexural strength of reinforced slabs compared to unreinforced weak slabs had a growth of 2 to 3 times and their displacements were limited.

1. Introduction

Several researchers have investigated different cementitious materials. One of these materials is high-performance fiber-reinforced cementitious composites (HPFRCC). HPFRCC has been classified based on the stress-strain behavior under tensile experiments. Some of the specifications of HPFRCC are multiple cracking behaviors, strain-hardening, and large energy absorption capacity [1–6]. On the other hand, High-performance concrete is a concrete sample that has special properties and characteristics, including strength, durability, strain hardening, and resistance against external aggressive factors. HPFRCC materials are classified separately from fiber-reinforced concrete (FRC) [7]. Although HPFRCC has good mechanical properties, it is not popular construction material. In general, in most studies on the use of cast-in-place HPFRCC materials, they have been used as wet mixtures to investigate the role of those materials in the improvement of the load-carrying capacity of beams, columns, and other structural elements. On the other hand, few researchers have used these materials [3-6].

In the case of the stress-strain curve of fiber-reinforced concrete, the softening strain occurs immediately after the first cracking. Therefore, it can be concluded that HPFRCC materials are a special type of fiber-reinforced concrete, which its tensile hardening behavior of tensile strain occurs after initial cracking, which is accompanied by multiple cracks until it reaches relatively high strains according to Fig. 1[1].

* Corresponding author. Tel.: +98-9193334438
E-mail address: zeinab1365_madah@yahoo.com

DOI: 10.22075/macs.2022.22215.1316
Received 2020-12-26; Received in revised form 2022-02-22; Accepted 2022-04-29.

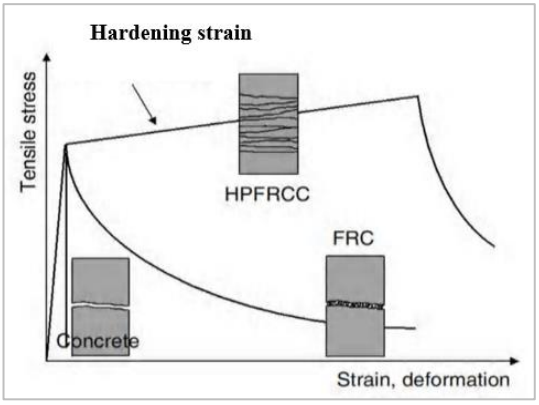

Fig. 1. Comparison of the tensile behavior of the conventional concrete, fiber-reinforced concrete, and HPFRCC [1]

Kortta fibers (Fig. 2) are one type of macro Synthetic fibers that consist of structural and non-structural polymeric composite fibers which are single-stranded. It is consisting of very fine strands of the copolymer and network fibers of polypropylene and Modified nanoparticle polypropylene. Fig. 2 shows macro-synthetic fibers of Kortta. The network fibers prevent the formation and expansion of surface cracks and primary cracks in concrete. The part of the intertwined strands after divergence in the concrete plays a role in preventing the formation of both primary and secondary cracks in hardened concrete [8].

Ilki in 2009 [9,10] used prefabricated HPFRCCs to strengthen columns through external confinement and observed that using precast HPFRCC panels for external confinement incremented the ductility and strength of strengthened columns under axial loads and reversed cyclic flexure and under the combined action of axial loads. In addition, in some investigations, the impact of HPFRCC and UHPFRCC materials has been applied in the form of a layer to study the flexural behavior of RC beams and slabs. In these investigations, several factors including the ratio of the longitudinal reinforcement, the impact of the a/d ratio, and the steel fibers volume fraction on the ultimate behavior, were studied [11–13].

Fig. 2. Korrta macro-synthetic fibers[8]

Hemmati et al. in 2015 [14] conducted experimental and parametric studies to evaluate the effect of compressive strength, load type, and tensile bar ratio on the characteristics of the ultimate displacement of reinforced HPFRCC beams. The results show that by using HPFRCC, the bearing capacity and ductility of these beams increased. They have also studied the rate of increasing the loading capacity of concrete frames reinforced with HPFRCC materials. In these specimens, the panel zone has been replaced with HPFRCC materials that have different tensile and compressive strengths. The results of full-scale concrete frames were compared with full-scale HPFRCC-reinforced concrete frames. The results show that by using these high-performance materials, the loading capacity and the ductility of these frames increase. Therefore, with the increasing compressive and tensile strength of these composite frames, the ductility of the frames had increased by 50 and 70%, respectively. Plastic hinges reached a maximum amount under the two-point loading [14].

Yang Zhang et al. in 2019 [15] studied capacity prediction and flexural behaviors on damaged RC bridge deck reinforced by layers of ultra-high performance concrete (UHPC). They evaluated cracking capacity, ultimate capacity, deformation features, and failure mode of RC-UHPC composites under positive bending moment and negative bending moment, respectively. The results showed that cracking and the ultimate capacity of composites experience an increase of nearly 2.5 and 2 times, in the given order, with UHPC situated on the tension surface compared with intact RC slab; While for UHPC at the compressive surface, no change in cracking capacity was recorded and ultimate capacity was 30% higher than that of the intact RC slab. In addition, stiffness increased with tensile stress in steel reinforcement in RC slabs, decreased after reinforcing for all specimens; and propagation of cracks in RC slabs was restrained and delayed because of the behavior of strain hardening and ultra-high ductility of UHPC [15].

Sharbatdar et al. in 2018 and 2019 [16,17] investigated the usage possibility of HPFRCC for reinforcing two-way reinforced concrete slabs. A total of five two-way slabs were constructed and tested to reach the rupture stage. One of the unreinforced slabs was selected as a control slab, and the rest of the slabs were reinforced in various forms. The reinforcements were carried out in two ways, once by installing veneer in the tensile area and once by installing veneer in both the tensile area and compression area each time with different percentages of the fibers. The behavior of bending and cracking, yielding and rupture of the laboratory samples were

evaluated. The results indicated that the installation of HPFRCC pre-fabricated laminates significantly improved the bending performance of reinforced slabs so that the ductility, energy absorption value, cracking strength, and initial hardness of the slabs were increased and the crack width was decreased. Therefore, the proposed precast HPFRCC sheets can be used to strengthen the deficient slabs [16,17].

Sabaghian et al. then in 2020 [18] conducted an investigation on the HPFRCC material to determine the mix proportion. HPFRCC laminates with and without longitudinal steel reinforcements were then tested. Finally, strengthened slabs were investigated by four-point flexural testing. The experimental results were suggestive of the effect of the properties of the HPFRCC laminate, including its application procedure, steel fiber volume fraction, incorporation of longitudinal reinforcement, and the type of reinforcement (steel or GFRP bars), on the increase in the load-bearing capacity of the slab. Adding longitudinal bars to the HPFRCC laminate improved the weaknesses of the crack pattern, load-carrying capacity, ductility, and stiffness. HPFRCC-laminate strengthening enabled a 92–326% increase in the load-bearing capacity of the slabs. This experimental undertaking is the first time that the HPFRCC laminate is reinforced with GFRP, successfully, with satisfactory results. Analytical models were developed to predict the flexural capacity of the one-way slab strengthened using HPFRCC laminate and the experimental results were compared to the predicted theoretical models. Analytical and experimental results showed excellent consistency with an average difference of 6% and a maximum of 18% [18].

In this study, the behavior of weak one-way concrete slabs was investigated. For more experimental studies, they were reinforced with precast HPFRCC Laminates of synthetic fiber type by NSM method. The obtained results are evaluated by the behavior of weak one-way concrete slab without reinforcement (weak reference specimen). For this purpose, 12 specimens of one-way concrete slabs with dimensions of 100 × 500 × 1140 mm were made so that the concrete mix design of all slabs was similar and the sound specimen which was considered as reference specimen (S) was reinforced with 4 longitudinal bars of No.8. In addition, the rest of the slabs were weakened by reducing the 4 longitudinal bars to 2 bars in the tensile zone. HPFRCC was produced with dimensions of 1000× 400× 30 mm with 1.5% and 3% synthetic fibers per cubic meter of mortar volume. These sheets were connected to the tensile zone of the concrete slab with the help of the NSM method. All slabs were tested by a three-point loading method with two fixed supports and a concentrated load in the middle of the span. The load-displacement results were shown in related diagrams and tables.

2. Material specifications

The used mix design is designed in the way that the average 28-day compressive strength is considered to be equal to 21 MPa for cylindrical specimens. Ordinary Portland cement of type 2 and washed sand and crushed grains of calcareous materials (with a maximum grain size of 12.5 mm) were considered in the mix design. Table 1 shows the mix design ratios of concrete materials per one cubic meter.

Table 1. The Mix design of 12 concrete slab specimens (per cubic meter)

Consumed materials	Sand	Pea gravel	Water	Portland cement (type 2)
Weight (kg)	835	1110	20+170	300

The water-to-cement ratio was considered to be 0.54, which is about 20 kg to saturate the dry materials. The concrete slump also measured about 76 mm. 6 standard cubic specimens with dimensions of 150×150×150 mm were made of the cast-in-place concrete mix to determine the actual strength of the concrete. The compressive strength of the concrete was determined using compression tests on cubic specimens. The specifications of cubic concrete specimens and the results of compressive strength were ranging from 22.94 to 24.12 MPa.

The compressive strength of the specimens was close to each other and provided the acceptance criteria for the specimens in accordance with the Iranian Concrete Regulations and ACI-318-14. The average 28-day compressive strength of the specimens was equal to 18.7 MPa based on the cylindrical specimen.

The steel bar was type AII and had an approximate yield strength of 300 MPa. The diameters of the used bars in the construction of the concrete slab were 6 and 8 mm. From each bar No. 6 and 8, 3 numbers with a length of 500 mm were selected for the tensile test. The results showed that the ultimate strength of bar No. 6 was 347.4 MPa and bar No. 8 was 500 MPa. The actual averages of yield strength of bars No. 6 and No. 8 were equal to 314.5 and 351.15 MPa obtained from uniaxial tensile tests, respectively.

According to the load-displacement test, the ultimate strain of steel bar (No.8) is equal to 0.176% by considering the modulus of elasticity equal to 200 GPa in accordance with Hook's law.

To ensure the complete interaction of the reinforcement materials of HPFRCC with concrete, epoxy adhesive with three-component

materials was used, which is a product of three components with high strength and high modulus of elasticity (in Table 2,3).

According to Fig. 2, the used fibers are of the type of korrta macro synthetic fibers. In this research, a short type of korrta fibers with a length of 19 mm has been used. It has been used in constructing HPFRCC Laminates with mortar weight ratios of 1.5 and 3%.

3. Mix design of precast reinforced materials of HPFRCC

The main components of concrete are one of the main factors in determining its mechanical properties. Grain size, grain surface roughness, the rate of porosity and void, the material containing aggregates, and the amount of absorbed water by aggregates are the main influential parameters in the characteristics of the concrete and their quality will directly affect the properties of the concrete. Concrete is containing a stone-like material that is a combination of cement, sand, sand, and water. The main mass of concrete is coarse and fine aggregates. The chemical interaction between cement and water, which covers the aggregates, causes the aggregates to integrate and stick to each other. The mixing design that was used to achieve a 28-day average compressive strength was designed on a cylindrical specimen (f_c= 21 MPa). Ordinary Type 2 Portland cement was used with clean sand and crushed calcareous aggregates with a maximum grain size of 12.5 mm. Table 4 shows the mixing design ratios of concrete materials per cubic meter.

The ratio of water to cement was considered to be 0.54. In addition, about 20 kg of excess water was used to saturate the dry material because a limited amount of water was needed to create a chemical reaction in cement, but the water used in the concrete mix is always much more than that. This excess water is used to create the necessary efficiency in the concrete to fill all the corners of the mold and around all the reinforcement rebars. The concrete slump was also measured at about 76 mm (Fig. 3).

In order to strengthen the flexural strength of one-way reinforced slabs and to make HPFRCC Laminates, macro synthetic fibers macro-synthetic fibers with a bulk ratio of 1.5% and 3%. Dry HPFRCC Laminates have dimensions of 1000 mm in length, 400 mm in width, and 30 mm in thickness (1000×400×30 mm). The weight of each sheet based on the mentioned dimensions was measured at an average of 21 kg, Fig. 4 shows a specimen of dry HPFRCC Laminates.

In order to make these Laminates, fine-grained sand materials with the nominal maximum size of aggregate of 4.75 mm and ordinary Portland cement of Type 2 and the water-to-cement ratio of 0.544 were used. Material weights of HPFRCC concrete with different percentages of fibers are recorded in Table 5.

Fig. 3. Measuring the concrete slump

Fig. 4. HPFRCC laminate

Table 2. Specifications of used epoxy adhesive

Type	Physical state	Specific gravity (kg/mm3)	7-day Tensile strength (MPa)	7-day Flexural strength (MPa)	7-day Compressive strength (MPa)
Epoxy	paste	0.167	17	38	95

Table 3. Specifications of korrta macro synthetic fibers [8]

Length (mm)	Diameter (μm)	Color	Tensile strength (MPa)	Modulus of Elasticity (MPa)	Density $\left(kg/dm^3\right)$	Chemical and Corrosion Resistance	Maximum Length Increase (%)	Water Absorption (%)
19-38-54	18	Gray	800	3500	0.9	Complete	10	0

Table 4. The mixing design of 12 samples of the concrete slab (per cubic meter)

Consumed material	Water	pea gravel	Sand	Cement (Type 2)
Weight (kg)	20 + 170	1110	835	300

Table 5. Material weights of HPFRCC concrete with 1.5 % and 3% synthetic fibers per cubic meter

Fiber	Gravel	Sand	Cement	Water
Bulk ratio	-	1	1	0.54

Table 6. Specifications of Compressive test specimens

No.	Compressive test specimen	Volume (mm^3)	Weight (kg)	Specific gravity (kg/mm^3)	Compressive strength of specimen (MPa)
1	HPFRCC1.5P	3375×10^3	7.26	2151.15×10^9	38.2
2	HPFRCC1.5P	3375×10^3	7.20	2133.30×10^9	38.5
3	HPFRCC1.5P	3375×10^3	7.18	2123.50×10^9	37.9
4	HPFRCC3P	3375×10^3	7.22	2141.20×10^9	40.9
5	HPFRCC3P	3375×10^3	7.26	2151.15×10^9	39.8
6	HPFRCC3P	3375×10^3	7.23	2144.30×10^9	42.12

The fibers were gradually added to the mortar to prevent the fibers from balling and accumulating in one part of the mortar.

After mixing the materials, a homogeneous and uniform mixture was obtained and then poured into molds made for this purpose and then cured. In order to measure the compressive strength of HPFRCC mortar, 3 cubic specimens of mortar with the dimensions of 150 × 150 × 150 mm and with a combination of 1.5% Korrta fibers were selected. 3 more specimens of mortar with the dimensions of 150 × 150 × 150 mm and with a combination of 3% of Korrta fibers were chosen. The average compressive strength was measured based on the standard cylindrical specimen for HPFRCC mortar with 1.5% fiber equal to 38.2MPa, while the average compressive strength of HPFRCC mortar with 3% fiber was equal to 41 MPa (Table 6).

3.1. Determining the type of slab

The desired slab is of one-way type due to the position of the slab supports in one direction. In this case, the slab acts in an orthogonal direction along with the supports.

3.1.1. Determining the minimum thickness and reinforcements of the slab

Due to the fact that the support conditions of the two ends of the slab are free, the minimum slab thickness according to ACI 318R-14 [19] is equal to L/20. It should be noted that this value is multiplied by the factor of (Fy / 700 + 0.4) for the case in which the yielding stress of steel and flexural stress of the slab is different from F_y=420MPa.

$$H_{min} = \frac{1}{20} \times (0.4 + \frac{fy}{700}) \quad (1)$$

which H_{min} is the minimum thickness of the slab based on mm and fy is yielding stress of steel based on MPa.

Given that the thickness of the slab is equal to 10 cm, then it corresponds to this value. The effective depth is equal to 76mm based on the following equation for φ8:

$$d = h - \left(cover + \frac{D}{2}\right) = 76\ mm \quad (2)$$

d is effective depth based on mm, h is the thickness of the slab based on mm is and D is the rebar diameter based on m.

The specimens were also checked for shear and the distance between the longitudinal reinforcements was obtained at 300 mm and the area of longitudinal reinforcement for a width of one meter is equal to 1.3908 cm^2 so 4φ8 is suitable.

4. Defining experimental specimens

12 full-scale specimens of one-way concrete slabs were constructed with the same geometric configuration. The dimensions of the specimens were 1140 mm long, 500 mm wide, and 100 mm thick (1140×500×100 mm). The specimens were designed with the purpose of increasing the bearing capacity and improving the flexural behavior in the reinforced specimens. In the reference specimen, the slab bars were arranged in a tensile layer and they were determined based on the ultimate load of 2 tons entered in the middle of the span.

Tie bars were provided by standard 180-degree bends at both ends of each bar. In order to provide temperature reinforcement in all slabs, 4 bars of No.6 were placed perpendicular to the longitudinal reinforcement and on the top of the reinforcement network at a distance of 250 mm. A view of the experimental specimens of the reference slab and the weak slabs and their reinforcement details are shown in Fig.5.

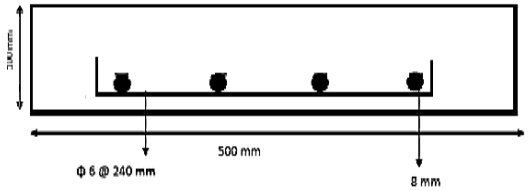

Fig. 5. Reinforcement details of concrete slab

The numbers and dimensions of grooves in weak slabs in Table 7 are referred to as specimens naming. Abbreviations were used to name concrete slab specimens according to Table 8. The arrangement of reinforcement slabs is shown in Fig.s 6 and 7.

Table 7. Concept of letters in naming concrete slab specimens

No.	Abbreviation	Concept
1	S	One Way Slab
2	SW	Weak Slab
3	R	Reinforcement
4	H	HPFRCC
5	N	Near Surface Mounted (NSM)
6	G	Groove

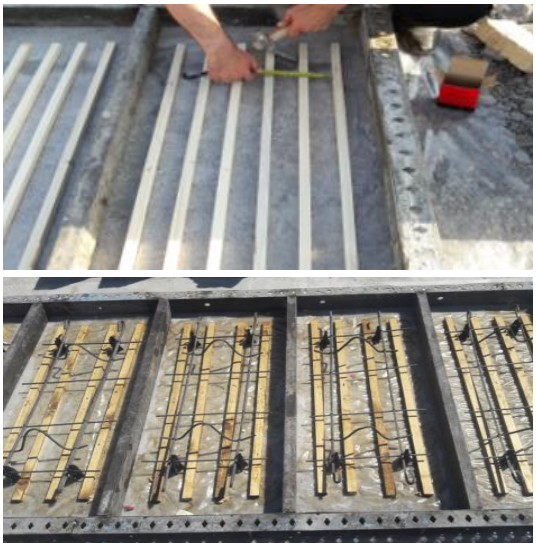

Fig. 6. Arrangement of reinforcement slabs

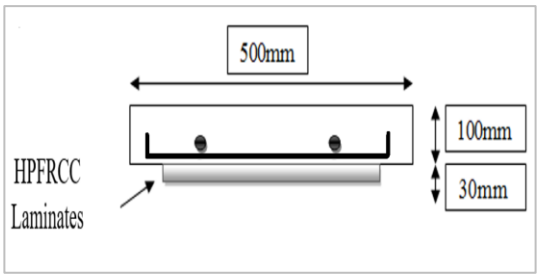

Fig. 7. Cross-section of the slab reinforced with HPFRCC Laminates

5. Analysis of the results of experiments

In this section, the results of the flexural test on reinforced and unreinforced on way concrete slabs were analyzed including load - displacement.

5.1. Analyzing the response of Load - displacement of specimens

The response of Load - displacement can be divided into two stages: before cracking and after-cracking stage can be divided into two sub-stages: the stage before hardening and the stage after hardening. The pre-yield cracking stage starts from the cracking load (P_{cr}) up to the yield load (P_y). The cracking stage after yielding starts from the yield load (P_y) up to the ultimate load (P_u).

Table 8. Names and the specifications of the tested slabs and the amount of reinforcement used in slabs

No.	Specimen name	Dimensions (mm)	Description	The weight of the tensile reinforcement of No.8 (kg)	Weight of temperature reinforcement of No.6 (kg)
1	S	1140×500×10	Sound Reference (S)	2.6	1.4
2	SW	1140×500×10	Weakened Reference (SW)	1.3	1.4
3	RSWH1.5PE	1140×500×10	Reinforced slab with a sheet having 1.5% fiber - without grooves	1.3	1.4
4	RSWH3PE	1140×500×10	Reinforced slab with a sheet having 3% fiber - without grooves	1.3	1.4
5	RSWH1.5PN2G6×2	1140×500×10	Reinforced slab with a sheet having 1.5% fiber and 2 grooves with 6 mm wide and 2 mm depth	1.3	1.4
6	RSWH3PN2G6×2	1140×500×10	Reinforced slab with a sheet having 3% fiber and 2 grooves with 6 mm wide and 2 mm depth	1.3	1.4
7	RSWH1.5PN4G2×3	1140×500×10	Reinforced slab with a sheet having 1.5% fiber and 4 grooves with 2 mm wide and 3 mm depth	1.3	1.4
8	RSWH3PN4G2×3	1140×500×10	Reinforced slab with a sheet having 3% fiber and 4 grooves with 2mm wide and 3 mm depth	1.3	1.4
9	RSWH1.5PN4G3×2	1140×500×10	Reinforced slab with a sheet having 1.5% fiber and 4 grooves with 3 mm wide and 2 mm depth	1.3	1.4
10	RSWH3PN4G3×2	1140×500×10	Reinforced slab with a sheet having 3% fiber and 4 grooves with 3 mm wide and 2 mm depth	1.3	1.4
11	RSWH1.5PN6G2×2	1140×500×10	Reinforced slab with a sheet having 1.5% fiber and 6 grooves with mm wide and 2 mm depth	1.3	1.4
12	RSWH3PN6G2×2	1140×500×10	Reinforced slab with a sheet having 3% fiber and 6 grooves with mm wide and 2 mm depth	1.3	1.4

*Grooves had the same lengths of 1000 mm but their width, depth, and numbers were different in every specimen.

The amount of load on which the armature is yielded was determined according to the relationship of ACI 318R-14 equal to 7.2 kN. Accordingly, the displacement corresponding to the load of 7.2kN was considered as Δ_y in the load-displacement diagram.

The ultimate load amounts of P_u and the ultimate displacement Δu after failure can also be recorded. If the loss rate of the load is more than 15% of the ultimate load in conventional concrete, the amount varies between 0.7 Pu and 0.85 Pu in HPFRCC reinforced concrete. In this research, the corresponding amount of the load is considered to be 0.8 Pu. After placing (Fig. 8) the specimen on two simple supports and placing the loading jack on the specimen with a uniform speed of 1MPa / min, it was statically loaded with a single-point concentrated load.

5.2. The response of Load - displacement of specimen RSWH3PE

As it can be seen from the response of Load – displacement of specimen RSWH3PE (Reinforced slab with a sheet having 3% fiber - without grooves) in Fig. 9, when the load and displacement, respectively, reached 24.90 kN and 4.26 mm, the failure occurred after significant yielding in flexural reinforcement materials and at the same time the specimen cracked.

At this stage, according to Fig. 10, the bridging action of fibers was observed in the HPFRCC laminate, which was associated with the rupture of fibers. Therefore, the load capacity of the specimen with a low slope decreased to 17.20 kN, which is equivalent to 70% of the ultimate load of 24.90 kN, and the displacement equivalent to this time was 11.35 mm. Therefore, the created crack in the middle of the span of the slab expanded and its width also increased. Then, the loading capacity of the specimen was gradually reduced So that in the displacement of 36.88 mm, the load was 13.64 kN and the crack width reached its maximum amount, which was 21.60 mm. After that, the specimen did not show any bending capacity, and the loading stage was completed.

Fig. 8. Laminate setup test

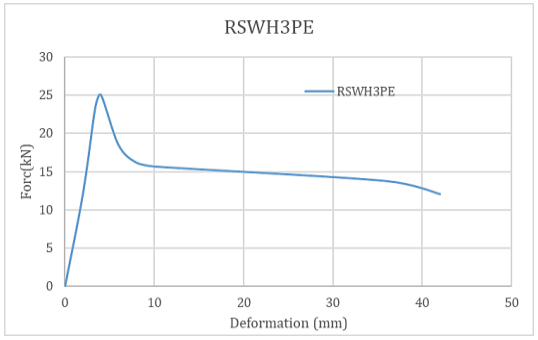

Fig. 9. Diagram of Load - displacement of specimen RSWH3PE

Fig. 10. Expanding the crack and increasing the crack width and bridging action of the fibers in specimen RSWH3PE

5.3. The response of Load – displacement of specimen RSWH3PN2G6×2

In this specimen, the weak reinforced concrete slab was arranged by 2 grooves with a width of 60 mm and a depth of 20 mm at equal distances on the bending surface. In this way, it can be provided a connection near the installation surface, so HPFRCC laminate with 3% fiber was attached to the bending surface of the slab with epoxy adhesive. According to Fig. 12, the created crack in the middle of the span has expanded and its width has also increased. As a result, the bearing capacity slowly decreased, again. So that in the displacement of 14.11 mm, the amount of load capacity was 8.80 kN (Fig. 11). After that, the specimen did not show any bending capacity, and the loading stage was completed.

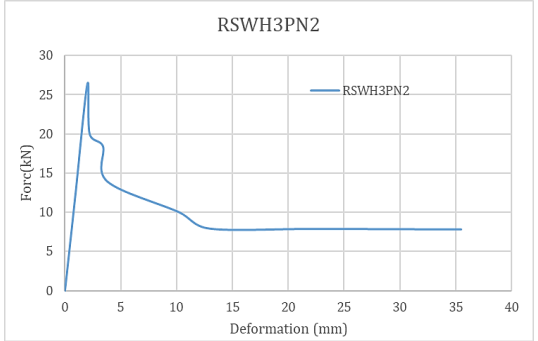

Fig. 11. Diagram of Load - displacement of specimen RSWH3PN2G6×2

Fig. 12. Expanding the crack and increasing the crack width and bridging action of the fibers in specimen RSWH3PN2G6×2

5.4. The response of Load – displacement of specimen RSWH3PN6G2×2

The weak reinforced concrete slab was arranged with 6 grooves with a width of 20 mm and a depth of 20 mm at equal distances on the bending surface. In this way, it can be a connection near to the installation surface, so HPFRCC laminate with 3% fiber was attached to the bending surface of the slab with epoxy adhesive. The load is equivalent to 61% of the ultimate load of 26.20 kN, and the displacement was equal to 6.9 mm at this time (Fig. 13).

The created crack in the middle of the span has expanded (Fig. 14) and its width has also increased so that the displacement reached 38.75 mm with a load capacity of 13.13 kN. After that, the specimen did not show any bending capacity and the loading stage was completed (Fig. 13).

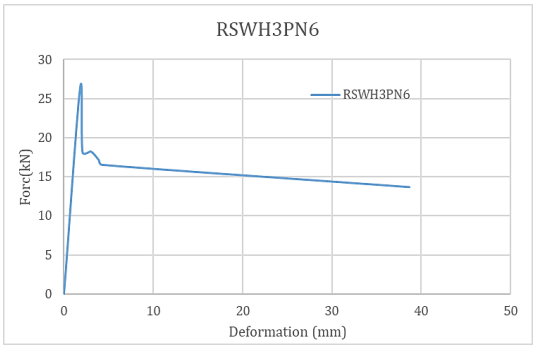

Fig. 13. Diagram of Load - displacement of specimen RSWH3PN6G2×2

Fig. 14. Expanding the crack and increasing the crack width and bridging action of the fibers in specimen RSWH3PN6G2×2

At all stages of loading, the HPFRCC reinforcement laminate was not separated from the concrete slab and the separation phenomenon did not occur. Due to the fact that the minimum load required to yield the rebar was 7.2 kN, it was predicted that the rebar would yield at the same time as the rupture of HPFRCC laminates happened, so the yielding load was considered equal to the ultimate load.

6. Comparison of load-deformation values of specimens

According to Fig. 16, which shows all the load-displacement curves of the tested specimens, a summary of the test results including the yield and ultimate loads and their corresponding displacement is provided for all specimens in Table 9.

In Fig. 15, it is observed that the response of the load-displacement of the control specimen, which included a stage before cracking, continued with an almost horizontal yield area resulting from yielding bars. As the applied load increased, the yielding gradually expanded until the specimen was broken in pure bending mode. In the reinforced specimens, the rupture occurred after significant yielding on precast laminates of HPFRCC and the total rupture occurred with a brittle behavior. The carrying capacity of all reinforced specimens decreased and the test was stopped.

Among the reinforced specimens, RSWH1.5PE, RSWH1.5PN4G2×3, and RSWH3PN4G2×3 showed more ductile behavior than other reinforced specimens (Table 9). The reinforced specimen of RSWH3PN6G2 × 2 had the lowest ductility among the reinforced specimens, and the behavior of this specimen was more brittle than the other specimens, and the load capacity of this specimen decreased at once.

Comparing the response of load-displacement of specimens in Fig. 15, it is observed that reinforcing by HPFRCC increased the cracking resistance and flexural stiffness of the specimens and significantly improved their bending capacity. An increase in cracking load in reinforced specimens compared to reference specimens is associated with the role of HPFRCC reinforcements in confining the expansion of cracks.

A comparison of the ultimate load values (P_u) for all 12 specimens, which are arranged by descending order and based on the ultimate load of the specimens, is shown in Fig.16. The weak reference specimen tolerated the lowest ultimate load (7.97 kN). All reinforced specimens had a higher bearing capacity than the reference specimen with an increased rate of 200% up to 330%.

The increase in cracking load observed in the reinforced slabs compared to the non-reinforced weak reference slab was attributed to the role of reinforcement of HPFRCC laminates in confining the expansion of cracks. The amount of rising in the ultimate load of the reinforced specimens was ranging from 1.1 to 4.26 mm due to the hardening effects of HPFRCC, which showed a significant decrease in comparison with the reference specimens.

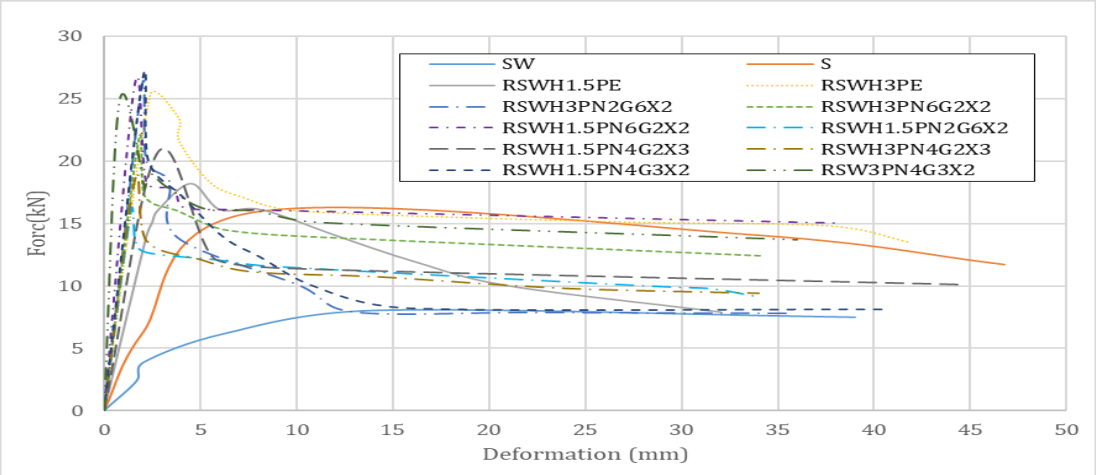

Fig. 15. Diagram of load-deformation of tested specimens

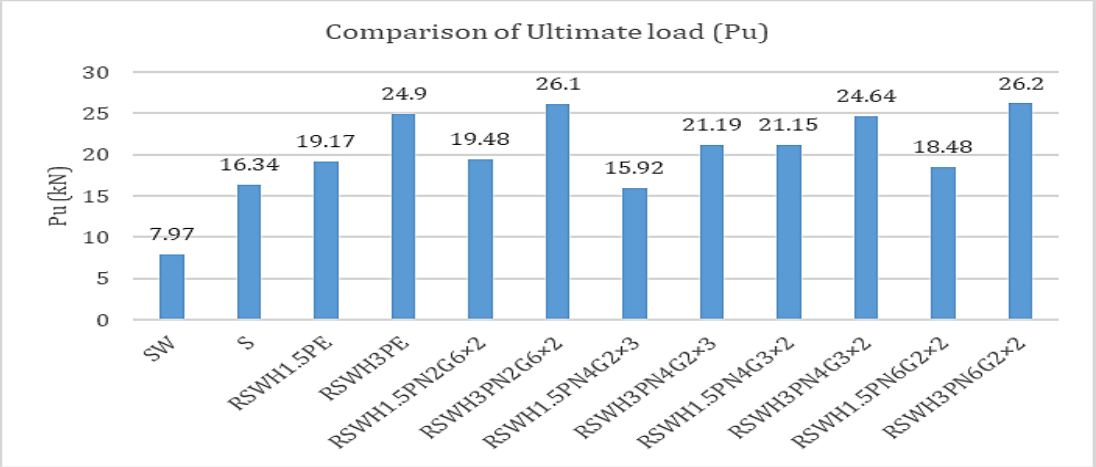

Fig. 16. Diagram of the ultimate load (Pu) of the specimens

Table 9. Summary of load-displacement results of experiments in the middle of the span

No.	Name of specimen	P_y (kN)	P_u (kN)	$P_{u80\%}$ (kN)	Δ_y (mm)	Δ_u[1] (mm)	$\Delta_{u80\%}$[2] (mm)	P_u / P_{usw} —	Δ_u / Δ_{usw} —	$\Delta_{u80\%} / \Delta_{u80\%sw}$ —	$\Delta_{u80\%} / \Delta_y$ —	Energy Absorption (kN.mm)
1	SW	6.77	7.97	6.37	5.35	20.80	48.95	1	1	1	9.15	322.0
2	S	14.92	16.34	13.43	6.13	11.85	38	2.05	0.60	0.78	6.20	545.0
3	RSWH1.5PE	19.17	19.17	15.42	4.01	4.01	11.02	2.40	0.2	0.22	2.75	186.0
4	RSWH3PE	24.90	24.90	19.43	4.26	4.26	5.55	3.12	0.21	0.11	1.30	88.7
5	RSWH1.5PN2G6×2	19.48	19.48	15.63	1.89	1.89	3.85	2.45	0.10	0.08	2.04	60.4
6	RSWH3PN2G6×2	26.10	26.10	20.88	1.89	1.89	2.40	3.27	0.10	0.05	1.27	39.3
7	RSWH1.5PN4G2×3	15.92	15.92	12.73	1.27	1.27	3.26	2	0.06	0.06	2.57	45.0
8	RSWH3PN4G2×3	21.19	21.19	16.83	1.15	1.15	2.87	2.65	0.05	0.06	2.50	52.4
9	RSWH1.5PN4G3×2	21.15	21.15	16.80	3.26	3.26	4.86	2.66	0.16	0.10	1.49	71.8
10	RSWH3PN4G3×2	24.64	24.64	19.71	1.27	1.27	1.85	3.10	0.06	0.04	1.46	31.4
11	RSWH1.5PN6G2×2	18.48	18.48	14.78	1.14	1.14	2.24	2.32	0.11	0.04	1.96	32.9
12	RSWH3PN6G2×2	26.20	26.20	20.96	1.06	1.06	1.32	3.30	0.04	0.05	1.24	21.4

[1] displacement of the slab center at the final load

[2] displacement of the slab center at 20 percent of load loss after ultimate load

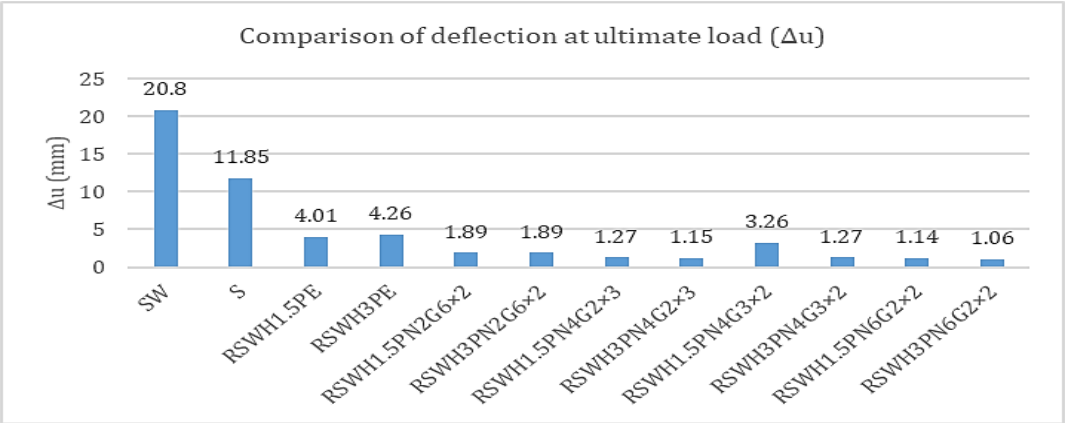

Fig. 17. Diagram of the deflection of specimens in the middle of the span at the moment of ultimate load (Δ_u)

In another comparison, the displacement corresponding to the ultimate load (Δ_u) for all 12 tested specimens is shown in descending order in Fig. 17. The amount of deflection in the ultimate load of the reinforced specimens was in the range of 1.1 and 4.26 mm due to the hardening effects of HPFRCC, which showed a significant decrease compared to the reference specimen. Among the reinforced specimens, the specimen RSWH3PN6G2×2 had the lowest deflection of 0.6 mm and the specimen RSWH3PE had the highest deflection corresponding to the ultimate load of 4.26 mm.

The maximum increase in load-bearing capacity of reinforced slab specimens in this study is compared with the obtained results of the research of ref. [18]. The rates of increasing load-bearing capacity of specimens in this research with Korrta fibers were equal to 99% in minimum amount and 229% in the maximum amount. For ref. [18] a maximum increase of 326% and a minimum increase of 92% at load carrying capacity had been obtained from the HPFRCC strengthened slabs reinforced with GFRP and steel laminates. Therefore, Korrta fiber also showed a significant increase in the load-bearing capacity of slabs compared to glass and steel fibers.

7. Analysis of the ductility of the displacement and the energy absorption in specimens

Ductility is defined as the ability of a structure to withstand non-elastic displacement after the first yielding displacement in steel bars so that there is no decrease in the load-bearing capacity of the structure. Ductility is introduced by a ratio called the Ductility factor (μ). The ductility factor is usually defined as the ratio of rotation (ϕ), curvature (χ), displacement (Δ), or absorbed energy (E) after the loss of 20% in the ultimate load to the corresponding values of the yielding load (according to Fig. 18 and Eq. 3).

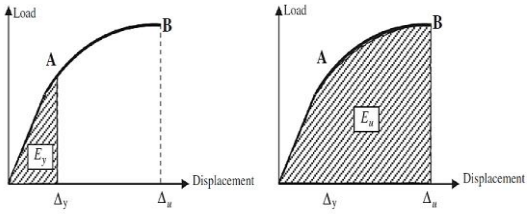

Fig. 18. Parameters of the displacement ductility and the energy ductility

In Fig. 19, for the response load-displacement curve of a reinforced concrete member, point A indicates the first yielding of the steel rebar and point B indicates the rupture of the member. Absorbed energy or Toughness is defined as the area under the load-displacement curve.

$$\mu_{\emptyset} = \frac{\emptyset_{u\,80\%}}{\emptyset_y} \tag{3}$$

$$\mu_{\chi} = \frac{\chi_{u\,80\%}}{\chi_y} \tag{4}$$

$$\mu_{\Delta} = \frac{\Delta_{u\,80\%}}{\Delta_y} \tag{5}$$

$$\mu_{\chi} = \frac{E_{u\,80\%}}{E_y} \tag{6}$$

A comparison of the amounts of absorbed energy and the displacement ductility and the energy ductility for all 12 specimens is given in Table 10. The bar diagram of the comparison of the displacement and energy ductility of the specimens is also shown in descending order in Fig. 19 and 20, respectively. As can be seen, the values of the displacement ductility for reinforced and reference specimens were between 1.24 and 9.15, so the highest displacement ductility belonged to the unreinforced reference specimen and the lowest displacement ductility belonged to the reinforced specimen RSWH3PN6G2×2. The energy ductility was between 1.24 and 8.8 so the highest energy ductility belonged to the unreinforced reference specimen and the lowest energy ductility belonged to the reinforced specimen RSWH3PN6G2×2.

Table 10. Summary of the results of the displacement and energy ductility in all specimens

NO.	Specimen	Δ_y (mm)	$\Delta_{u80\%}$ (mm)	μ_Δ	$\mu_\Delta / \mu_{\Delta control}$	E_y (kN.mm)	$E_{u80\%}$ (kN.mm)	μ_E	$\mu_E / \mu_{Econtrol}$
1	SW	5.35	48.95	9.15	1	17.7	155.9	8.8	1
2	S	6.13	38	6.2	0.67	45.7	248.33	5.4	0.61
3	RSWH1.5PE	4.01	11.02	2.75	0.3	38.43	113.58	2.95	0.33
4	RSWH3PE	4.26	5.55	1.3	0.14	53.03	69.09	1.3	0.14
5	RSWH1.5PN2G6×2	1.89	3.85	2.04	0.22	18.4	37.5	2.04	0.23
6	RSWH3PN2G6×2	1.89	2.4	1.27	0.13	26.66	31.32	1.17	0.13
7	RSWH1.5PN4G2×3	1.27	3.26	2.57	0.28	10.1	25.94	2.57	0.29
8	RSWH3PN4G2×3	1.15	2.87	2.50	0.27	12.18	30.4	2.5	0.28
9	RSWH1.5PN4G3×2	3.26	4.86	1.49	0.16	34.47	50.39	1.46	0.16
10	RSWH3PN4G3×2	1.27	1.85	1.46	0.16	15.64	22.79	1.45	0.16
11	RSWH1.5PN6G2×2	1.14	2.24	1.96	0.21	10.53	20.64	1.96	0.22
12	RSWH3PN6G2×2	1.06	1.32	1.24	0.13	13.88	17.26	1.24	0.14

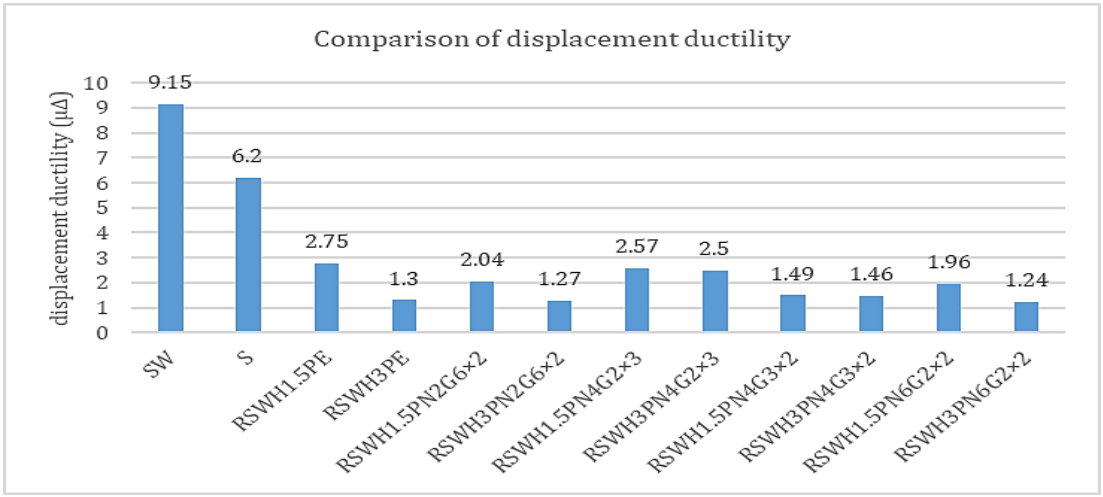

Fig. 19. Diagram of the displacement ductility in all specimens

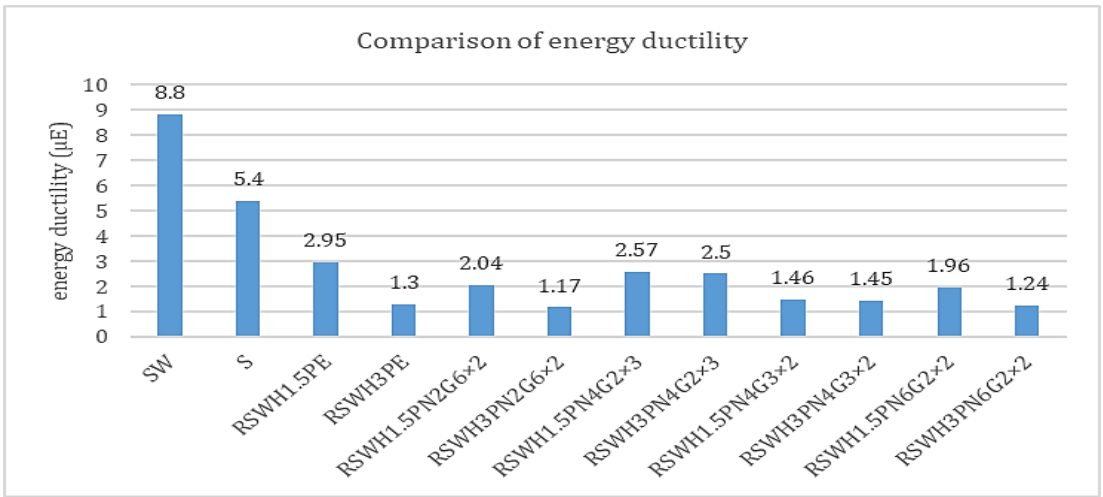

Fig. 20. Diagram of the energy ductility in all specimens

It is observed that in the specimens that had a higher ductility, the bearing capacity decreased smoothly and was not accompanied by a sudden decrease. Conversely, specimens with a lower ductility showed more brittle behavior, and their bearing capacity of them fell at once.

In addition, the reference specimens had the highest amount of deformation and energy ductility among all specimens. The RSWH1.5PE and RSWH1.5PN2G6 × 2 specimens had the highest amount of ductility among the reinforced specimens but had lower ductility than the reference specimen. The RSWH3PN6G2 × 2 specimens had the lowest amount of ductility among the specimens. In general, it can be said that the specimens reinforced with 1.5% fiber provided better ductility than the specimens reinforced with 3% fiber.

8. Conclusion

Based on the experimental results of reference specimens and weak flexural slabs reinforced with HPFRCC laminates, the following results are compiled:

The experimental results showed that the use of HPFRCC laminates was a feasible and useful method for flexural reinforcement of one-way reinforced concrete with low cover. With the use of three partial epoxy adhesives, it was possible to prevent the separation of stuck external HPFRCC laminates from the concrete surface.

Due to the fact that in non-grooved specimens, the separation of reinforcement materials did not occur until the end of loading and rupture of the specimen so it was possible to avoid grooving the slabs, which was a time-consuming action and expensive and led to an increase in the consumption of the adhesive.

All of the reinforced specimens with HPFRCC laminates had a higher bearing capacity than the non-reinforced weak reference specimens with an increased rate of between 200 and 330%.

The increase in strength of reinforced specimens depended on the percentage of fiber used in the construction of HPFRCC laminates so that the incremental rate of the strength in specimens reinforced with 3% fiber laminates compared to specimens reinforced with 1.5% fiber with similar specifications is between 20 and 35%.

The amount of rising the ultimate load of the reinforced specimens was ranging from 1.1 to 4.26 mm due to the hardening effects of HPFRCC, which showed a significant decrease in comparison with the reference specimens.

The specimens reinforced with 1.5% fiber provided better ductility than the specimens reinforced with 3% fiber.

The amount of ductility and also the response diagram of load-displacement of specimens are directly related to their failure mode. Generally, an increase in the flexural capacity of the specimens is associated with a decrease in their ductility.

Due to the comparison between the bearing capacity of reinforced specimens and the normal references specimen, it can be concluded that the reinforcement method with HPFRCC laminates was able to increase the flexural strength of weak specimens higher than the flexural bearing surface of the normal specimen, which could be seen in all reinforced specimens. HPFRCC laminates compensated for the flexural weakness Caused by the reduction of the capacity of the slab tensile bars.

References

[1] Naaman, A.E., and Reinhardt, HW., 2003. Setting the stage: toward performance-based clasentsification of FRC composites. *In High Performance Fiber Reinforced Cement Composites* (HPFRCC-4), Proceeding of the 4th Int'l RILEM Workshop.

[2] Li, V.C., Stang, H., Krenchel, H., 1993. Micromechanics of crack bridging in fibre-reinforced concrete. *J. Mater Struct,* 26:486–94.

[3] Hemmati, A., Kheyroddin, A., Sharbatdar, M.K., 2015. Increasing the flexural capacity of RC beams using partially HPFRCC layers. *J. Comput Concr,*16 :545–68.

[4] Abbaszadeh, M.A., Sharbatdar, M.K., Kheyroddin, A., 2017. Performance of two-way RC slabs retrofitted by different configurations of high performance fiber reinforced cementitious composite strips. *The Open Civil Engineering Journal,* 11:650–63.

[5] Fallah, M.M., Sharbatdar, M.K., Kheyroddin, A., 2019. Experimental strengthening of the two-way reinforced concrete slabs with high performance fiber reinforced cement composites (HPFRCC) prefabricated sheets. *J Rehabil Civ Eng*; 7:1–17.

[6] Naaman, A.E., Reinhardt, H.W., 2007. Proposed classification of HPFRC composites based on their tensile response. *J Mater Struct* ;39:547–55.

[7] Ferrari, V.J., De Hanai, J.B., De Souza. R.A., 2013. Flexural strengthening of reinforcement concrete beams using high performance fiber reinforcement cement-based composite (HPFRCC) and carbon fiber reinforced polymers (CFRP). *J Constr Build Mater*; 48:485–98.

[8] Pourjahanshahi, A., Madani, H., 2021. Chloride diffusivity and mechanical performance of UHPC with hybrid fibers under heat treatment regime, *Materials Today Communications,* 26, p.102146.

[9] Ilki, A., Yılmaz, E., Demir, C., Kumbasar, N., 2004. Prefabricated SFRC Jackets for Seismic Retrofit of Non-Ductile Rectangular Reinforced Concrete Columns. *13th World conference on earthquake engineering, Vancouver*, BC, Canada.

[10] Ilki, A., Demir, C., Bedirhanoglu, I., Kumbasar, N., 2009. Seismic retrofit of brittle and low strength RC columns using fiber reinforced polymer and cementitious composites. *J. Adv. Struct. Eng*; 12:325–47.

[11] Yang, J.M., Min, K.H., Shin, H.O., Yoon, Y.S., 2012. Effect of steel and synthetic fibers on flexural behavior of high-strength concrete beams reinforced with FRP bars. *J. Compos Part B Eng.*, 43:1077–86.

[12] Tanarslan, H.M., 2017. Flexural strengthening of RC beams with prefabricated ultra-high performance fibre reinforced concrete laminates. .*J Eng. Struct,* 151:337–48.

[13] Tanarslan, H.M., Alver, N., Jahangiri, R., Yalçınkaya, Ç., Yazıcı, H., 2017. Flexural strengthening of RC beams using UHPFRC laminates: bonding techniques and rebar addition, *Construction and Building Materials,* 155:45–55.

[14] Hemmati, A., Kheyroddin, A., and Sharbatdar,M. K., 2015. Plastic Hinge Rotation Capacity of Reinforced HPFRCC Beams. *ASCE J. Struct. Eng*., 141(2), 04014111.

[15] Zhang, Y., Zhu, Y., Yeseta**,** M., 2019. Flexural behaviors and capacity prediction on damaged reinforcement concrete (RC) bridge deck strengthened by ultra-high performance concrete (UHPC) layer. *CIVIL, ARCHITECTURAL AND ENVIRONMENTAL ENGINEERING FACULTY RESEARCH & CREATIVE WORKS*, ISSN-0950-0618.

[16] Fallah Bafghi, M., Sharbatdar, M.K., Kheyroddin, A., 2018. Experimental study of the performance of two-way RC slabs retrofitted with high performance fiber reinforced cement composite (HPFRCC) prefabricated laminates. in Persian, *Journal of Structural and Construction Engineering*, DOI:10.22065/jsce.2018.120672.148.

[17] Fallah Bafghi, M., Sharbatdar, M.K., Kheyroddin, A., 2019. Improving ductility and strength of two-way RC Slabs strengthened with HPFRCC prefabricated sheets, *Journal of Rehabilitation in Civil Engineering*, Volume 7, Issue 4, Serial Number 16, pp. 1-17, DOI: 10.22075/JRCE.2018.14532.1266.

[18] Sabbaghian, M., Kheyroddin, A., 2020. Flexural strengthening of RC one way slabs with high-performance fiber reinforced cementitious composite laminates using steel and GFRP bar, *Engineering Structures* 221 (2020) 111106.

[19] ACI 318-19, 2019. Building code requirements for structural concrete and commentary. *ACI Standard and Report 11*.